Supporting Information

6FDA-DAM Polyimide-Based Mixed Matrix Membranes with Functionalized UiO-67 Nanoparticles for improved CO_2 Separation Performance

Mohammad Hadi Nematollahi[a], Joaõ A. P. Coutinho[a], Reza Abedini[b,*], and Pedro J. Carvalho[a,*]

[a] CICECO - Aveiro Institute of Materials, Department of Chemistry, University of Aveiro, Aveiro 3810-193, Portugal

[b] EOR & Gas Processing Research Lab, Faculty of Chemical Engineering, Babol Noshirvani University of Technology, Babol 4714871167, Iran

*Corresponding author: quijorge@ua.pt (Pedro J. Carvalho), abedini@nit.ac.ir (R. Abedini)

Monomers purification

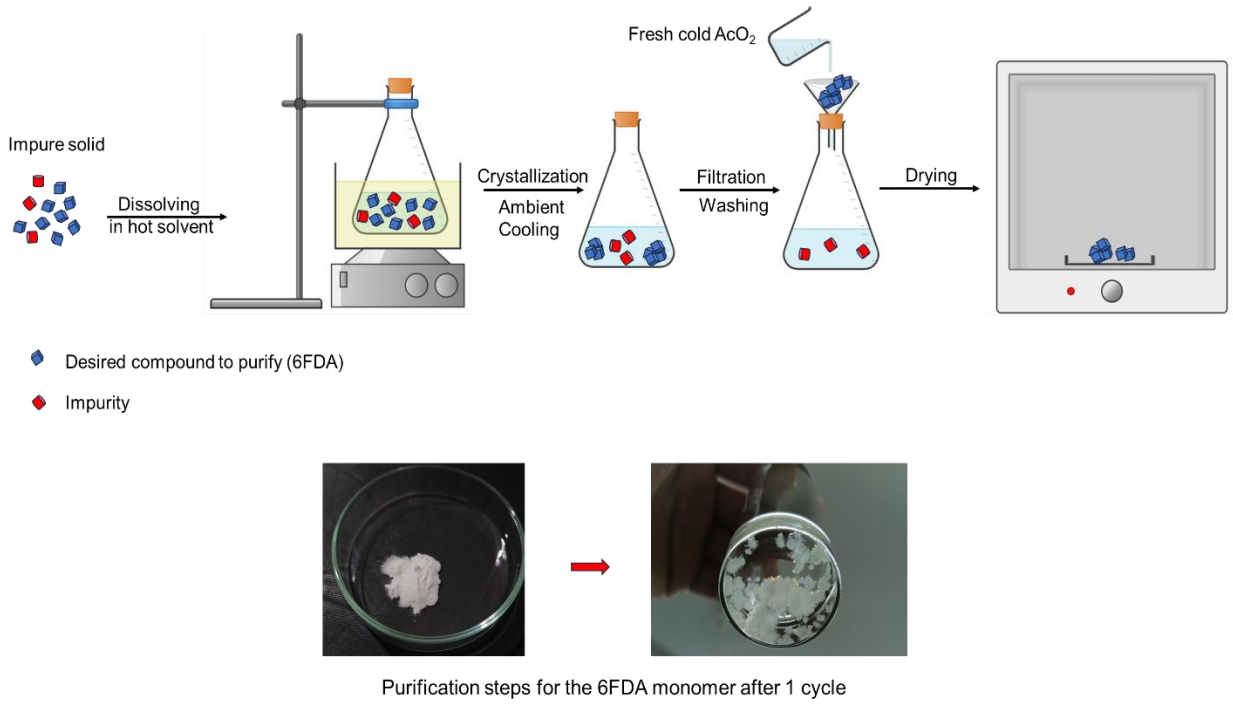

Purification steps for the 6FDA monomer after 1 cycle

Scheme S 1. Recrystallization of 6FDA monomer

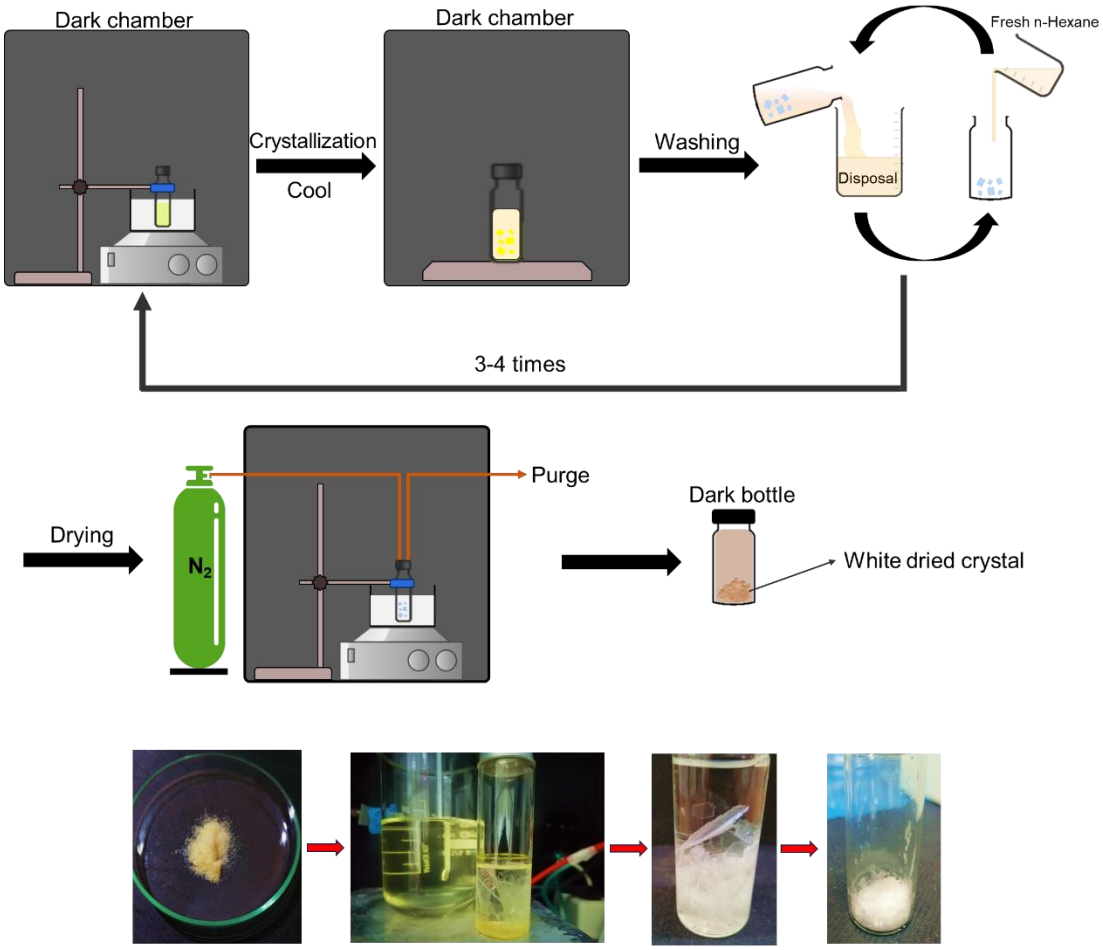

Purification steps for the DAM monomer after 4 cycles

Scheme S 2. Recrystallization of DAM monomer

Gas permeation experiment

Before each measurement, all lines and cell chambers were initially vacuumed via a pump, and then the target gas was introduced into the top retentate chamber (still without contact with the membrane). After temperature stabilization, the gas was allowed to get in contact with the membrane, and the permeate side pressure increment was recorded with a pressure sensor with an accuracy of 1 mbar. The permeability was then, determined through:

$$P = \frac{273.15 \cdot 10^{10} \cdot v \cdot l}{A \cdot T \cdot (76 \cdot p_0)} \left(\frac{\partial p}{\partial t}\right) \quad \text{(S1)}$$

where P is the gas permeability in Barrer (1 Barrer = 10^{-10} cm^3 (STP). cm. cm^{-2}. s^{-1}. $cmHg^{-1}$), v the permeate chamber volume (cm^3), T the temperature (K), l the membrane thickness (cm), A the membrane's actual surface area (cm^2), p_0 the retentate side pressure, and $\left(\frac{\partial p}{\partial t}\right)$ the slope of the pressure changes with time (atm/s) in the steady state gas permeation.

The ideal permselectivity of gas i over gas j (α_{ij}) can be determined by:

$$\alpha_{ij} = \frac{P_i}{P_j} \quad \text{(S2)}$$

The time lag method was used to determine the diffusion coefficients (D) as follows:

$$D = \frac{l^2}{6\theta} \quad \text{(S3)}$$

where θ is the time lag (delay time) (s). The solution-diffusion mechanism was considered valid in gas transport through self-standing membranes. According to this model, the permeability of each gas through the polymeric membrane is the multiplication of the gas diffusivity (10^{-8} [$cm^2.s^{-1}$]) and solubility (10^{-2} [cm^3 (STP) cm^{-3} $cmHg^{-1}$]). Therefore, the solubility coefficient (S) is determined as follows:

$$S = \frac{P}{D} \quad \text{(S4)}$$

Structural characterization of UiO-67 and its derivatives

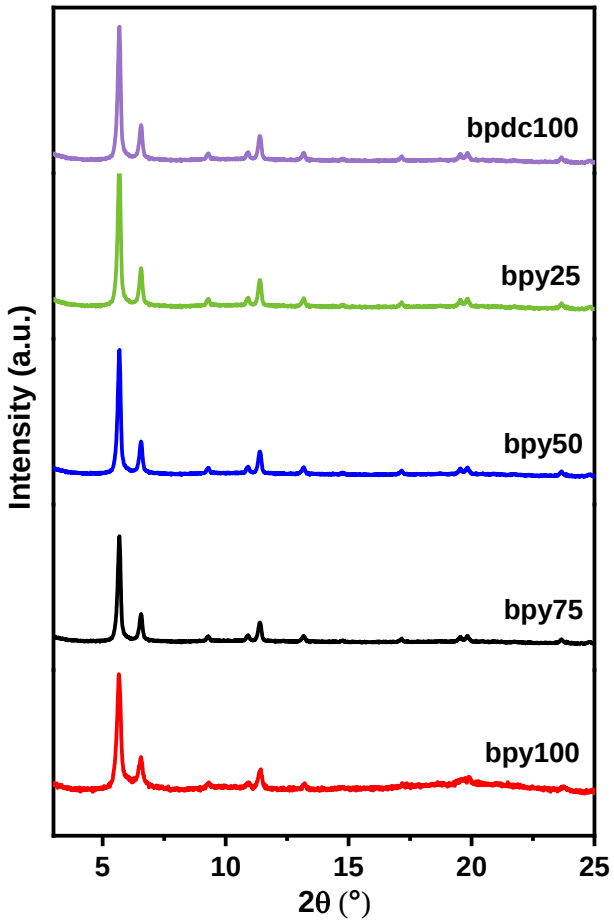

Figure S 1. XRD pattern of all powders.

Table S 1. BET analysis and textural properties of UiO-67s powders.

Sample	Surface area ($m^2.g^{-1}$)			Pore volume ($cm^3.g^{-1}$)			Mean pore diameter (D_p) (nm)
	S_{BET}	S_{Micro}	S_{Meso}	V_{Total}	V_{Micro}	V_{Meso}	
bpdc100	2018	1862	156	0.91	0.73	0.18	2.034
bpy25	1925	1690	235	0.92	0.68	0.24	2.025
bpy50	1883	1813	70	0.99	0.74	0.250	2.242
bpy75	1854	1793	61	0.97	0.73	0.24	2.07
bpy100	1799	1640	159	0.93	0.64	0.29	2.235

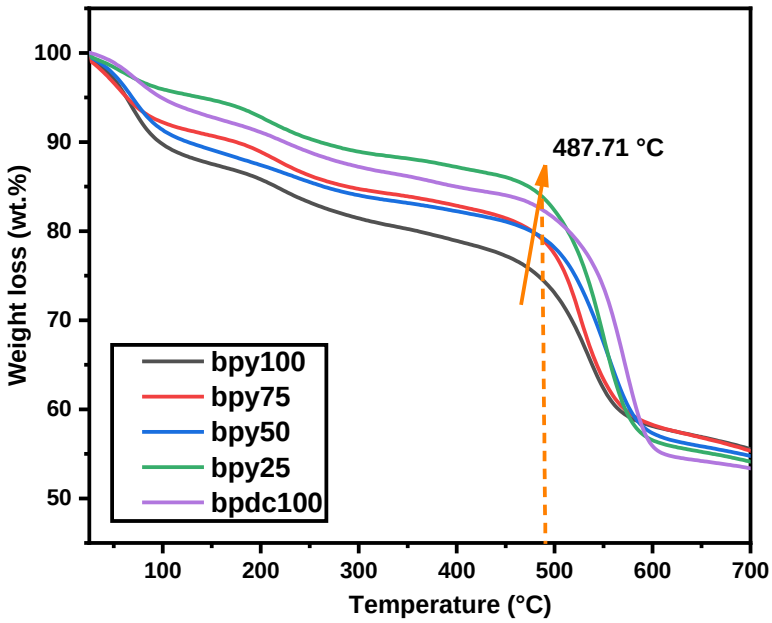

Figure S 2. TGA curves of all the studied powders.

Structural characterization of MMMs

Table S 2. The Bragg d-spacings values of the synthesized MMMs

Sample codes	2θ (°)	d-spacing (*Å*)
PPI	13.83	6.40
PPI-1	11.88	7.44
PPI-2	11.63	7.60
PPI-3	12.13	7.29
PPI-4	12.4	7.13
PPI-5	12.7	6.96

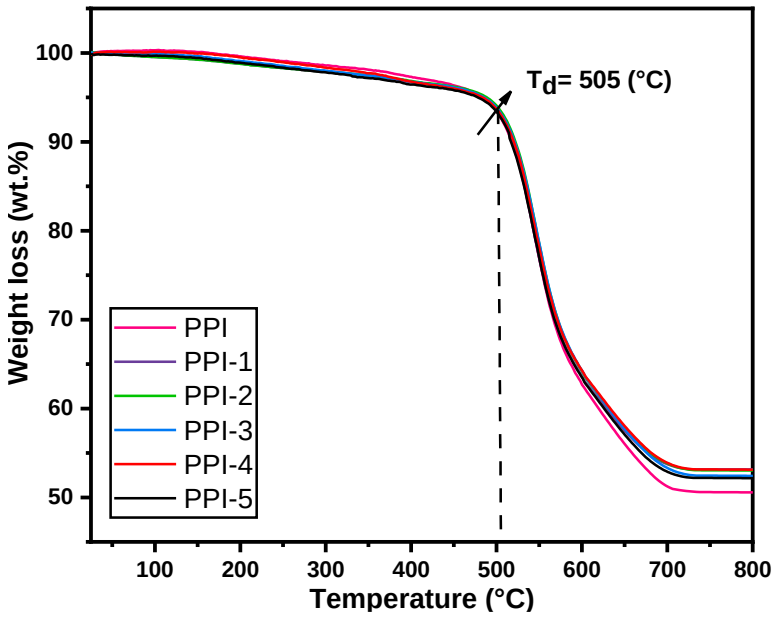

Figure S 3. TGA curves of the prepared MMMs.

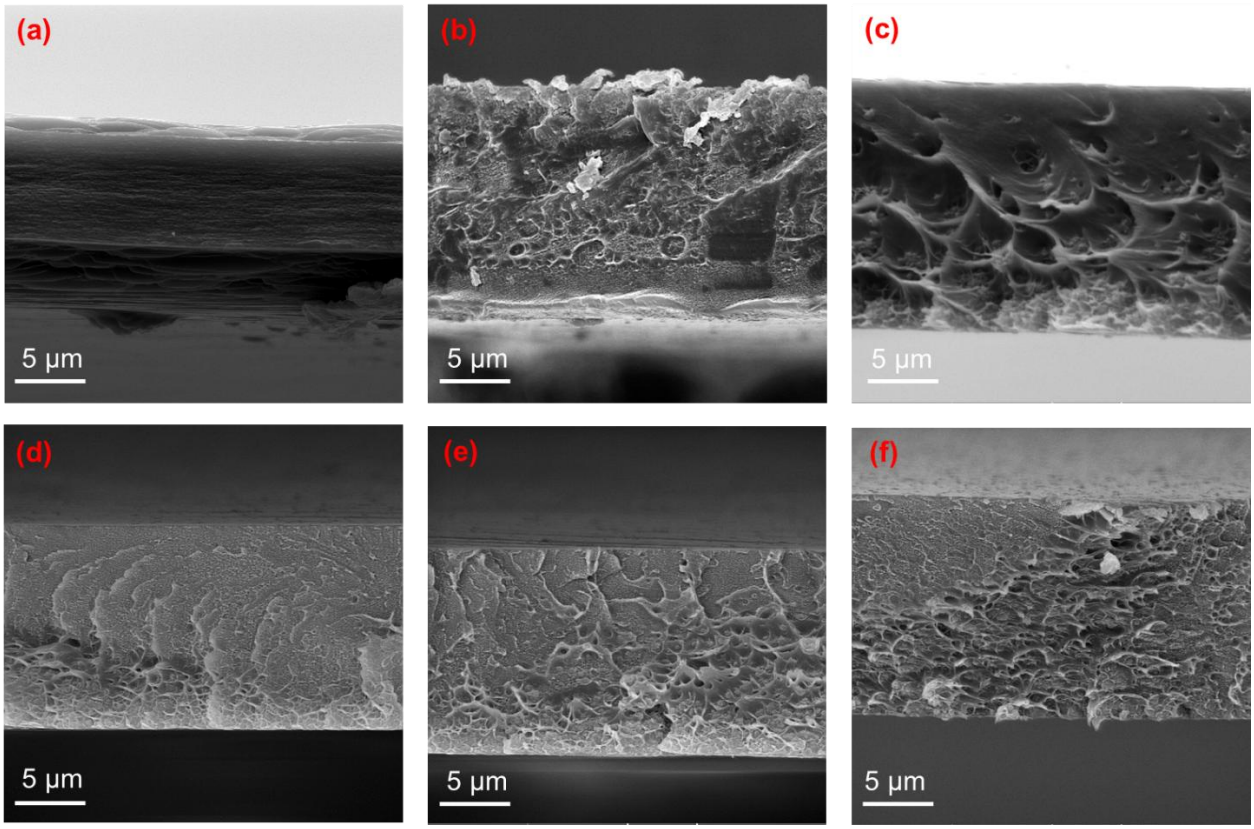

Figure S 4. Cross-sectional images of (a) PPI, (b) PPI-1, (c) PPI-2, (d) PPI-3, (e) PPI-4, and (f) PPI-5 membranes.

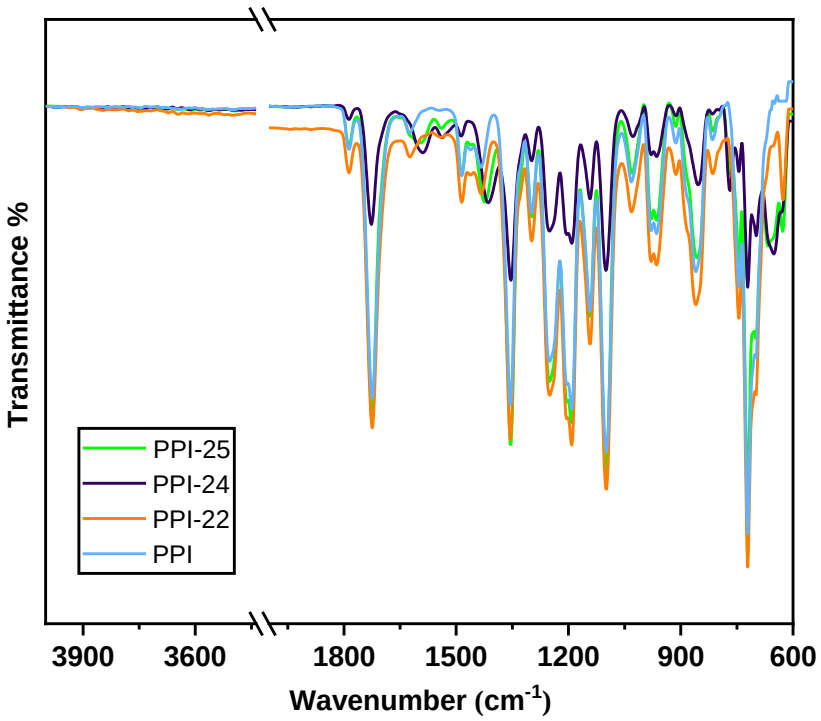

Figure S 5. ATR of bpy25-based MMMs

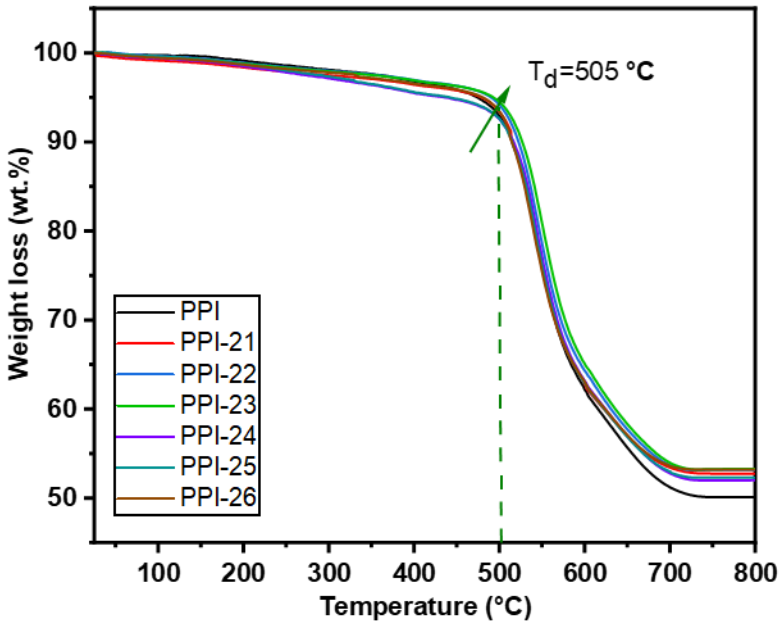

Figure S 6. TGA curves of bpy25-based MMMs.

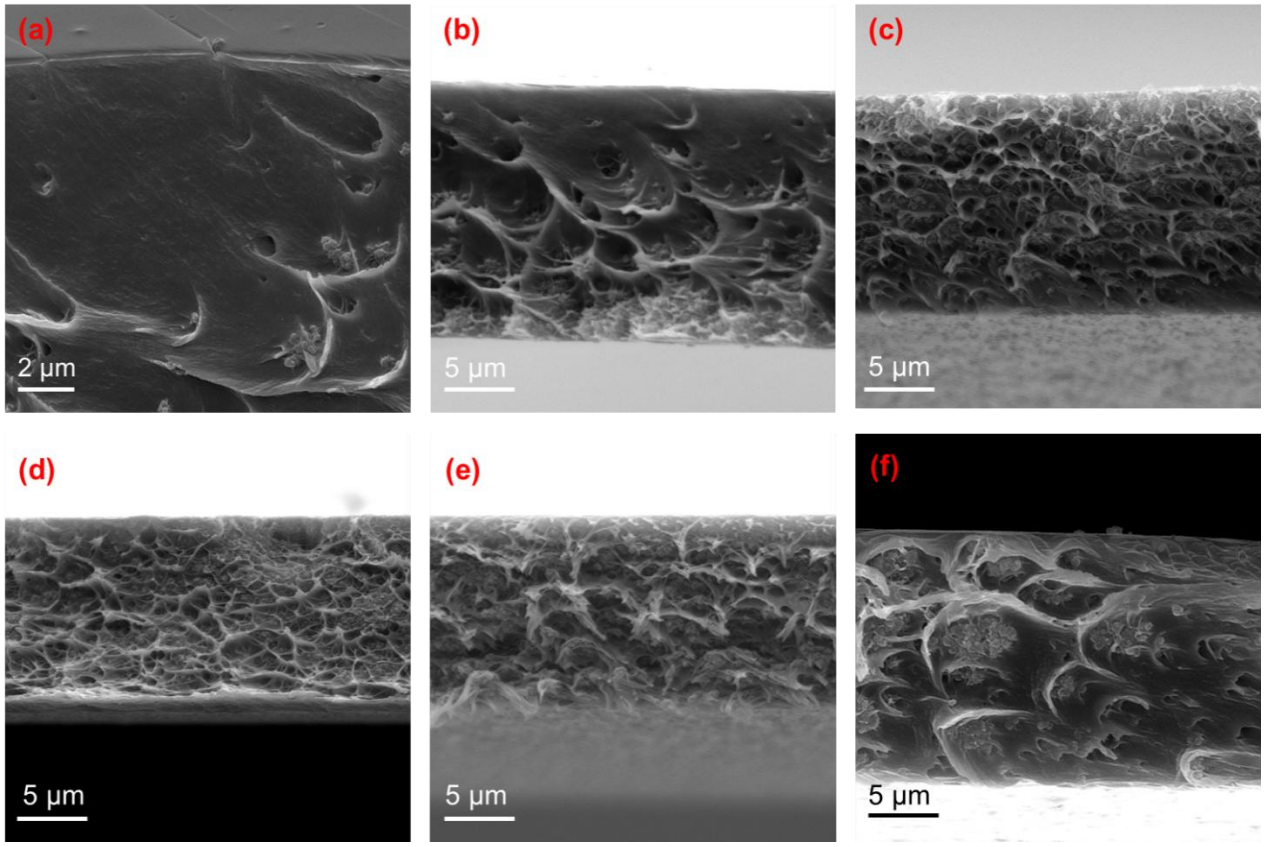

Figure S 7. Cross-sectional images of (a) PPI-21, (b) PPI-22, (c) PPI-23, (d) PPI-24, (e) PPI-25, and (f) PPI-26 membranes.

Performance of the developed MMMs

Table S 3. Comparison of CO_2/CH_4 and CO_2/N_2 separation performance of reported membranes and the experimental data obtained in this study.

Polymer	Additive (*wt.*%)	Test condition (*T*(°C)/*p*(bar))	P_{CO2} (Barrer)	Selectivity		Ref.
				CO_2/CH_4	CO_2/N_2	
Matrimid	–	25/3	8.01[a]	37.3	–	[1]
	MIL-53-NH_2 (8)		9.03	36.5		
	MIL-53-NH_2 (16)		7.39	41.8		
6FDA-DAM	–		358.45	31.22		
	MIL-53-NH_2 (5)		431.58	31.14		
	MIL-53-NH_2 (10)		463.56	30.53		
	MIL-53-NH_2 (15)		581.78	29.00		
	MIL-53-NH_2 (20)		659.73	28.00		
Matrimid5218	–	30/5	16.2	38	–	[2]
	UiO-66 (10)		26	40		
	UiO-67 (10)		24	55		
	UiO-67-33[b] (10)	30/4	27	75		
6FDA-Durene	–	35/2	805.3[a]	20	–	[3]
	ZIF-67 (30)		1463.7	15.5		

	VZIF-67 (30)		1210	32.51		
6FDA-Durene	–	35/3.5	959	16.4	14.7	[4]
	ZIF-71 (10)		1805	16.1	14.9	
	ZIF-71 (20)		4006	12.8	12.9	
	ZIF-71 (30)		7750	9.53	11.5	
			917[a]	21.8	–	
			1606	20		
			3435	16		
			5642	9.2		
6FDA-Durene	–	25/2	455.21	–	14.02	[5]
	ASZX (5)		637.3		19.17	
	ASZX (10)		772.65		22.19	
	ASZX (15)		887.31		25.34	
	ASZX (20)		925.16		19.86	
6FDA-Durene	–	35/5	1131.91	19.61	–	[6]
	ZIF-90 (45)		3946.23	6.93		
	ZIF-90-NH_2 (45)			17.36		
6FDA-DAM: DABA (3:1)	–	35/2	199[a]	35.9	–	[7]
	SSZ-16[c] (5)		365	34.8		
	SSZ-16 (10)		340	28.6		
	SSZ-16 (15)		315	16.2		
6FDA-DAM: DABA (3:2)	–	35/4.5	150.5	27.5	–	[8]
	Glycidol (27)		145.8	29.6		
	Glycidol (41)		94.6	32.7		
	–	35/6.9	158.9[a]	37.8		
	Glycidol (27)		149.1	38.3		
	Glycidol (41)		95.6	39.1		
6FDA-DAM: DABA (3.2)	–	35/1.01	134.01	38.3	23.3	[9]
	DMS (10)		202.09	36.2	22.2	
	DMS (20)		364.96	33	20.8	
6FDA-DAM	–	35/3	1237[a]	35.7	–	[10]
	S13_sph&sh[d] (10)		829	26.8		
	S13_sheet_RT(10)		824	32		
	–		1245	–	20.4	
	S13_sph&sh (10)		761		21.3	
	S13_sheet_RT(10)		633		21	
6FDA-DAM	–	35/3	1503[a]	26	–	[11]
	–		1566	–	20.1	
	ZIF-8 (10)		1962	18.4	–	
	ZIF-8 (10)		2310	–	18.3	
6FDA-DAM/PIM-1(10 wt.%)	–		2135	25	–	
	–		2184	–	21.4	
	ZIF-8 (10)		2891	26.6	–	
	ZIF-8 (10)		2802	–	18.1	
	ZIF-8 (20)		2396	19	–	
	ZIF-8 (20)		1648	–	16.3	
6FDA-DAM	–	25/2	503	–	13.8	[12]
	–		714[a]		23.8	

	ZIF-94 (10)		865		24.8	
	ZIF-94 (20)		1070		22.9	
	ZIF-94 (30)		1125		19.7	
	ZIF-94 (40)		2165		22.4	
6FDA-DAM	–	25/1	590[a]	30	–	[13]
	ns-CuBDC[e] (2)		570	37		
	ns-CuBDC (4)		430	43		
6FDA-DAM	–	25/4	603	19.4	–	[14]
	ZIF-301 (20)		825	24.9	–	
PIM-1	–		4000	–	15	[15]
	DMOF-1[b](10)		7000		13	
	DMOF-1-Azo(10)		7500		19	
	DMOF-1-Azo(20)		10000		17	
PIM-1	–		7500		14	[16]
	UiO-66		13000		14	
	UiO-66-Azo[b] (16.7)		13000		16	
	UiO-66-Azo (33.3)		13000		14	
	UiO-66-Azo (66.7)		11000		14	
	UiO-66-Azo (100)		11000		19	
6FDA-DAM	–	30/2	723.7	24.4	30.59	This work
	bpdc100 (10)		944.26	29.06	35.17	
	bpy25[b] (10)		1024.3	35.32	44.15	
	bpy25 (20)		1298.85	41.3	50.68	

a: mixed gas, b: mixed-ligand approach, c: aminosilanized zeolite 13X, d: this new ZIF named UZAR-S13 is formed by Zn^{2+} and 4(5)-(hydroxymethyl)imidazolate. UZAR-S13 has two distinct phases: amorphous spheres and sheet crystals, e: 2-D CuBDC nanosheets,

Reference

(1) Sabetghadam, A.; Seoane, B.; Keskin, D.; Duim, N.; Rodenas, T.; Shahid, S.; Sorribas, S.; Guillouzer, C. L.; Clet, G.; Tellez, C. Metal organic framework crystals in mixed-matrix membranes: impact of the filler morphology on the gas separation performance. *Advanced functional materials* **2016**, *26* (18), 3154-3163.

(2) Thür, R.; Van Velthoven, N.; Slootmaekers, S.; Didden, J.; Verbeke, R.; Smolders, S.; Dickmann, M.; Egger, W.; De Vos, D.; Vankelecom, I. F. Bipyridine-based UiO-67 as novel filler in mixed-matrix membranes for CO_2-selective gas separation. *Journal of Membrane Science* **2019**, *576*, 78-87.

(3) Chen, K.; Ni, L.; Zhang, H.; Xie, J.; Yan, X.; Chen, S.; Qi, J.; Wang, C.; Sun, X.; Li, J. Veiled metal organic frameworks nanofillers for mixed matrix membranes with enhanced CO_2/CH_4 separation performance. *Separation and Purification Technology* **2021**, *279*, 119707.

(4) Japip, S.; Wang, H.; Xiao, Y.; Chung, T. S. Highly permeable zeolitic imidazolate framework (ZIF)-71 nano-particles enhanced polyimide membranes for gas separation. *Journal of Membrane Science* **2014**, *467*, 162-174.

(5) Mashhadikhan, S.; Amooghin, A. E.; Moghadassi, A.; Sanaeepur, H. Functionalized filler/synthesized 6FDA-Durene high performance mixed matrix membrane for CO_2 separation. *Journal of Industrial and Engineering Chemistry* **2021**, *93*, 482-494.

(6) Li, G.; Si, Z.; Yang, S.; Zhuang, Y.; Pang, S.; Cui, Y.; Baeyens, J.; Qin, P. A defects-free ZIF-90/6FDA-Durene membrane based on the hydrogen bonding/covalent bonding interaction for gas separation. *Journal of Membrane Science* **2022**, *661*, 120910.
(7) Ahmad, M. Z.; Izak, P.; Fila, V. CO_2 separation of fluorinated 6FDA-based polyimides, performance-improved ZIF-incorporated mixed matrix membranes and gas permeability model evaluations. *Journal of Environmental Chemical Engineering* **2022**, *10* (6), 108611.
(8) Eguchi, H.; Kim, D. J.; Koros, W. J. Chemically cross-linkable polyimide membranes for improved transport plasticization resistance for natural gas separation. *Polymer* **2015**, *58*, 121-129.
(9) Park, S.; Bang, J.; Choi, J.; Lee, S. H.; Lee, J.-H.; Lee, J. S. 3-Dimensionally disordered mesoporous silica (DMS)-containing mixed matrix membranes for CO2 and non-CO2 greenhouse gas separations. *Separation and Purification Technology* **2014**, *136*, 286-295.
(10) Perea-Cachero, A.; Sánchez-Laínez, J.; Berenguer-Murcia, Á.; Cazorla-Amorós, D.; Téllez, C.; Coronas, J. A new zeolitic hydroxymethylimidazolate material and its use in mixed matrix membranes based on 6FDA-DAM for gas separation. *Journal of Membrane Science* **2017**, *544*, 88-97.
(11) Sánchez-Laínez, J.; Pardillos-Ruiz, A.; Carta, M.; Malpass-Evans, R.; McKeown, N. B.; Téllez, C.; Coronas, J. Polymer engineering by blending PIM-1 and 6FDA-DAM for ZIF-8 containing mixed matrix membranes applied to CO_2 separations. *Separation and Purification Technology* **2019**, *224*, 456-462.
(12) Etxeberria-Benavides, M.; David, O.; Johnson, T.; Łozińska, M. M.; Orsi, A.; Wright, P. A.; Mastel, S.; Hillenbrand, R.; Kapteijn, F.; Gascon, J. High performance mixed matrix membranes (MMMs) composed of ZIF-94 filler and 6FDA-DAM polymer. *Journal of membrane science* **2018**, *550*, 198-207.
(13) Yang, Y.; Goh, K.; Wang, R.; Bae, T.-H. High-performance nanocomposite membranes realized by efficient molecular sieving with CuBDC nanosheets. *Chemical Communications* **2017**, *53* (30), 4254-4257.
(14) Wang, Z.; Yuan, J.; Li, R.; Zhu, H.; Duan, J.; Guo, Y.; Liu, G.; Jin, W. ZIF-301 MOF/6FDA-DAM polyimide mixed-matrix membranes for CO_2/CH_4 separation. *Separation and Purification Technology* **2021**, *264*, 118431.
(15) Prasetya, N.; Ladewig, B. P. New Azo-DMOF-1 MOF as a photoresponsive low-energy CO_2 adsorbent and its exceptional CO_2/N_2 separation performance in mixed matrix membranes. *ACS applied materials & interfaces* **2018**, *10* (40), 34291-34301.
(16) Prasetya, N.; Ladewig, B. P. An insight into the effect of azobenzene functionalities studied in UiO-66 frameworks for low energy CO_2 capture and CO_2/N_2 membrane separation. *Journal of Materials Chemistry A* **2019**, *7* (25), 15164-15172.